



## Soil formation and organic matter accretion in a young andesitic chronosequence at Mt. Shasta, California

Juliane Lilienfein<sup>a</sup>, Robert G. Qualls<sup>a,\*</sup>, Shauna M. Uselman<sup>a</sup>,  
Scott D. Bridgham<sup>b</sup>

<sup>a</sup>*Department of Environmental and Resource Sciences, University of Nevada-Reno, 1000 Valley Road, Reno, NV 89557, USA*

<sup>b</sup>*Department of Biology, University of Notre Dame, Notre Dame, IN 46556, USA*

Received 12 September 2002; accepted 29 January 2003

### Abstract

The objectives of this work were to study rates of increase in allophane concentration, specific surface area changes, and organic matter accretion in a young andesitic chronosequence. We sampled the 0–10-, 10–20-, 30–40-, 70–80-, and 140–150-cm depths of 77-, 255-, 616-, and approximately 1200+-year-old soils and analyzed them for allophane, ferrihydrite, specific surface area, cation exchange capacity, soil pH, and C and N concentrations. Allophane concentrations increased at rates up to a maximum of  $0.14 \text{ g kg}^{-1} \text{ year}^{-1}$ , and concentrations are up to 68 times higher in the oldest than in the youngest soil. During the same time ferrihydrite concentrations increased only by a factor of 2.3. The specific surface area that could be attributed to allophane was only 2–4% in the youngest soil but was 41–97% in the oldest soil. Carbon and N stocks increased linearly with soil age over the first ~ 600 years with rates of  $139 \text{ kg C ha}^{-1} \text{ year}^{-1}$  and  $5.3 \text{ kg N ha}^{-1} \text{ year}^{-1}$ , respectively. After about 600 years, accretion rates were lower. Increases in allophane concentrations lead to increased cation exchange capacity in the soil. Our results indicate that the ability of the soil to retain nutrients improved with soil development.

© 2003 Elsevier Science B.V. All rights reserved.

*Keywords:* Allophane; Soil organic matter accretion; Soil chronosequence; Specific surface area

\* Corresponding author. Fax: +1-775-784-4789.

E-mail address: [qualls@unr.edu](mailto:qualls@unr.edu) (R.G. Qualls).

## 1. Introduction

Soil chronosequences are a valuable tool for investigating rate and direction of pedogenic changes (Hugget, 1998). The Mt. Shasta mudflow soil chronosequence has served as a classical example of soil development and primary succession (Jenny, 1980; Schlesinger, 1997). These changes that occur during soil development fundamentally affect the biogeochemical cycling in the ecosystem. Although organic matter accretion has been studied in the Mt. Shasta mudflow chronosequence (Dickson and Crocker, 1953b; Sollins et al., 1983), mineralogical changes have not yet been studied in detail.

Allophane, a group of short-range order minerals, which contain Al and Si in specific combination, is a mineral typically occurring in young volcanic soils (Wada, 1989). The Al or Si composition of allophane depends on the weathering and leaching conditions during allophane formation. Aluminum-rich allophane (Al/Si=2) is normally formed where the soil solution is relatively poor in Si, while Si-rich allophane (Al/Si=1) is formed at higher Si concentrations (Parfitt, 1990). Higher Si concentrations normally occur in drier climates or under restricted leaching conditions. Aluminum-rich allophane (Al/Si=2) occurs more frequently and is probably more stable under leaching conditions than other types of allophane (Parfitt and Kimble, 1989). In an andesitic chronosequence of Costa Rica, Nieuwenhuys et al. (2000) found that allophane concentrations are highest in an 18,000-year-old soil and lower in a 2000- and 450,000-year-old soil. But due to uncertainties about soil ages and differences in climate between soils of different ages, conclusions about the formation rates of allophane are difficult. Due to the high specific surface area of allophane of 435 to 534 m<sup>2</sup> g<sup>-1</sup> (Wada, 1989) and its capacity for adsorption, surface area of the soils may change significantly during soil formation and this may have consequences for the ability of the soil to prevent nutrient or pollutant leaching from the soil.

Although organic matter accretion in the Mt. Shasta mudflows has been treated in two studies (Dickson and Crocker, 1953b; Sollins et al., 1983), there is still uncertainty about the accretion rates. Binkley et al. (2000) reviewed several studies of N accretion rates during primary succession to evaluate the existence of “occult” N input, which included the Mt. Shasta mudflows. The estimates ranged between 5 and 63 kg N ha<sup>-1</sup> year<sup>-1</sup>, depending on the author of the study, what soil ages were compared, and what N concentration was assumed for the parent material at the time of deposition. Binkley et al. (2000) concluded that the best evidence suggested an N accretion rate of 5–10 kg N ha<sup>-1</sup> year<sup>-1</sup>.

Binkley et al. (2000) describe three approaches to assess N accretion in forest soils: paired plots, chronosequences, and repeated sampling of individual sites, each with their limitations. In our study, we have the unique opportunity to combine a chronosequence study with repeated sampling of an individual site by combining our data with those from Dickson and Crocker (1953b) and Sollins et al. (1983) who all measured C and N concentrations in the soils. This gives us the possibility to study the C and N concentrations in 27-, 55-, 77-, 255-, 616-, and approximately 1200+-year-old soils. Therefore we were able to perform time series evaluation with the help of linear regression or curve fitting, which Binkley et al. (2000) suggested as a more powerful tool to calculate accretion rates than the comparison of only two data points from repeated sampling or chronosequence studies.

The objectives of this work were to study (1) the rate of allophane and ferrihydrite formation, surface area, and cation exchange capacity with regard to the consequences for adsorption and leaching of nutrients, and (2) to clarify the controversy with regard to C and N accretion rates by adding additional data and combining the repeated sampling and the chronosequence approach.

## 2. Materials and methods

### 2.1. Study sites

The study was performed in the Mt. Shasta Mudflow Research Natural Area (RNA) in northern California, about 6 km northeast of McCloud, CA. The soils in the area were formed on cold volcanic mudflows of coarse sandy andesitic material, which originated from the south slope of Mt. Shasta. Topography and current climate are similar across the chronosequence. As all mudflows originate from one common canyon on the south side of the mountain, parent material of all flows is similar in chemical composition (Sollins et al., 1983). The parent material originates from below a glacier (approximately 3000 m above sea level) so that the material coming down the mudflows was chemically unweathered beyond that caused by volcanism. Therefore, chemical weathering and soil formation started after the material had been deposited. The parent material of all flows consists of ground rocks of hornblende–andesite composition (Dickson and Crocker, 1953a). The constituents of the fine sand fraction (100–250  $\mu\text{m}$ ), in order of decreasing concentration, are as follows: plagioclase, volcanic rocks, hyperstene, volcanic glass, hornblende, and augite (Dickson and Crocker, 1953a).

Although the history of the flows is not completely established (Sollins et al., 1983), the age of at least three of the four flows is well established. The most recent flow (A flow) occurred in 1924 and 1926 so that at our sampling time in 2001 the soil was about 77 years old. Dickson and Crocker (1953a) distinguished four other older flows (B through E) and determined the age of the B, C, and D flow by the age of the oldest trees found growing upon the actual surface of each deposit, and which were not growing on any buried soil below. As the age of the oldest soil, the E flow, exceeded the life span of trees, the age was estimated by comparing the morphological characteristics of a portion of the E flow that was buried by the D flow. They concluded that the soil was at least older than the 616-year-old D-flow soil and was arbitrarily designated as 1200+ years. Glauser (1967) estimated the age of the B flow to  $450 \pm 200$  years based on  $^{14}\text{C}$  dating of a tree buried in the mudflow. After having thoroughly investigated the soil profiles in the B- and C-flow area, we believe that the B and C flows are the same and the age is that which Dickson and Crocker estimated in 1953 to be 205 years. We conclude that in 2001 the ages of the soils were the following: A: 77, B+C: 255, D: 616, and E: 1200+ years old.

As the Mt. Shasta mudflow chronosequence is a young chronosequence compared to other chronosequences (Nieuwenhuysen et al., 2000), all soils developed under similar climatic conditions. All plots are within an area of 10 km<sup>2</sup> and between 1300 and 1350 m a.s.l. Therefore, the current climatic conditions of all flows are also similar. Meko et al. (2001) reconstructed the climate in northern California after 869 A.D. using tree-ring data

and concluded that long-term precipitation averages were similar throughout the study period. In general, the climate can be described as a winter precipitation–summer drought temperate climate (Dickson and Crocker, 1953a). The average annual precipitation in the last 50 years was about 1300 mm, from which about 80% fell during the 5-month period between November and March, mainly as snow. The average annual temperature during the last 50 years was 9.9 °C, varying between 1.4 °C in January and 20 °C in July. The average daily maximum ranged between 8 and 3 °C, and the average daily minimum between –5 and 9 °C (weather data collected at McCloud, CA, 6 km away). All soils are well-drained and dry to less than 5% volumetric water content at 1.5 m soil depths during the summer months (unpublished data).

The vegetation differs with the age of the flows and has been described by Dickson and Crocker (1953a) and Glauser (1967). The youngest stand in A flow is mainly Ponderosa pine (*Pinus ponderosa* Dougl. ex Laws). The older stands are composed predominantly of Ponderosa pine, Incense cedar (*Calocedrus decurrens* Torr.), White fir (*Abies concolor* [Gord. and Glend.] Lindl. ex Hildebr.), Sugar pine (*Pinus lambertiana*), and California black oak (*Quercus kelloggii* Newb.). Sollins et al. (1983) reported that shrubs (*Arctostaphylos patula* Greene, *Ceanothus* spp., and *Purshia tridentata* (Pursh.) DC) and grasses increase with importance with age of the flows, whereas amounts of *Pteridium aquilinum* (L.) Kuhn decrease.

## 2.2. Sampling

For the sampling we established transects in the A, D, and E flows. Because the B flow exists only as separate “islands”, no transects were established but plots were allocated randomly. We attempted to locate our transects close to where Sollins et al. (1983) sampled. In each of the flows we established five to six plots, which were randomly chosen along the transects. Certain areas where the soil profiles were not deep enough or where the area was obviously disturbed by fire or bark beetles were rejected. Soil samples for chemical analyses were taken from the 0–10-, 10–20-, 30–40-, 70–80-, and 140–150-cm layers. For the 0–10- and 10–20-cm soil depth, three samples were taken per plot, which were composited for analyses.

## 2.3. Bulk density measurement and stock calculations

To determine the bulk density of the fine (<2 mm) fraction we took undisturbed samples with a bulk density corer from each plot. We were unable to obtain intact bulk density samples for the 140–150-cm depth but the bulk density data was only used for calculating C and N stocks to the 70-cm depth. Soil samples were dried at 40 °C and sieved to separate the <2-mm and >2-mm fractions. The volume of the coarse fraction in the bulk density cores (>2 mm) was determined by measuring the displacement of water.

The bulk density of the fine soil (<2 mm) was calculated as follows:

$$\text{Bulk density}_{\text{fine soil}} = \frac{\text{mass}_{\text{fine soil}}}{(\text{volume}_{\text{whole soil}} - \text{volume}_{\text{coarse fraction}})} \quad (1)$$

To determine the volume of the coarse fraction, we dug soil pits and weighed the mass of the moist soil in the following soil layers: 0–10, 10–20, 30–40, and 40–80 cm. Afterwards,

the soil was sieved to <12 mm to homogenize the soil. Subsamples were dried (40 °C) and sieved to <2 mm. The volumes of the 2–12-mm fraction and the >12-mm fraction were measured by displacement of water to calculate the total volume of the >2-mm fraction.

Stocks of C for each soil layer were calculated as follows:

$$C \text{ stock} = 100 * C \text{ conc}_{fs} * D * BD_{\text{fine soil}} * (100 - V_{cf}) / 100 \quad (2)$$

Where C stock is expressed in kg ha<sup>-1</sup> for the depth increment *D* in cm, *BD<sub>fine soil</sub>* is the bulk density of the fine soil in g cm<sup>-3</sup>, *V<sub>cf</sub>* is the volume of the coarse fraction in % and 100 is the unitless conversion factor to obtain kg ha<sup>-1</sup>. The stock of N was also calculated accordingly. To obtain the C and N stocks for the 0–70-cm soil depth, we summed the stocks of each individual soil layer.

#### 2.4. Chemical analyses

Soil samples for chemical analyses were dried at 40 °C and passed through a 2-mm sieve for homogenization. Soil pH was measured in water with a soil/solution ration of 1:1. Average pH was calculated as the arithmetic average pH value according to Baker et al. (1981). Organic C and N content was determined on ground subsamples by dry combustion with a Perkin Elmer 2400 CHN analyzer (Perkin Elmer, NJ). Ammonium oxalate extractable Al, Fe, and Si (*Al<sub>o</sub>*, *Fe<sub>o</sub>*, and *Si<sub>o</sub>*) were determined by the method of Schwertmann (1964), dithionate–citrate–bicarbonate extractable Fe (*Fe<sub>d</sub>*) by the method of Holmgren (1967), and pyrophosphate extractable Al (*Al<sub>p</sub>*) by the method of McKeague (1967). Metal concentrations in the extracts were determined using inductively coupled plasma emission spectroscopy. Effective cation-exchange capacity (*CEC<sub>eff</sub>*) was determined by saturating the soil with 0.2 M NH<sub>4</sub>Cl solution, then washing the entrained solution with water, and then extracting with 0.2 M KCl solution (Sumner and Miller, 1996). Exchanged NH<sub>4</sub><sup>+</sup> was measured with a flow injection analyzer (QuikChem 8000, Lachat).

Concentrations of crystalline Fe oxides were calculated as follows:

$$Fe_{\text{cryst}} = Fe_d - Fe_o \quad (3)$$

Allophane concentrations, in terms of g kg<sup>-1</sup> soil, can be calculated by the following equation as summarized by Dahlgren (1994):

$$\text{Allophane} = f * Si_o \quad (4)$$

The factor *f* depends on the Si/Al molar ratio and distinguishes Si-rich allophane (Al/Si, 1:1) and Al-rich allophane or imogolite (Al/Si, 2:1). Factor *f* can be determined as follows:

$$f = (Al_o - Al_p) / Si_o \quad (5)$$

For an Al/Si ratio of 1:1, the factor is 5, for one of 2:1 the factor is 7.

Ferrihydrite concentrations were calculated as (Parfitt and Childs, 1988):

$$\text{Ferrihydrite} = 1.7 * \text{Fe}_o \quad (6)$$

Specific surface area was determined by the ethylene glycol monoethyl ether (EGME) method according to Carter et al. (1986). EGME is assumed to form a monomolecular layer on all interlayer and external surfaces. The weight increase of soil samples exposed to EGME can therefore be used to estimate the specific surface area of soil samples:

$$A = W_a(W_s * 0.000286) \quad (7)$$

Where  $A$  is the specific surface area in  $\text{m}^2 \text{g}^{-1}$ ,  $W_a$  is the weight of EGME in g,  $W_s$  is the weight of soil in g, and 0.000286 is the weight in g of EGME required to form a monomolecular layer on a square meter surface.

### 2.5. Statistical evaluation

Statistical differences among groups were tested with analysis of variance (ANOVA), and between pairs of data with Student's  $t$ -test. Statistical analyses were performed with MS Excel.

## 3. Results and discussion

### 3.1. Mineralogical analyses

All dithionate, oxalate, and pyrophosphate extractable Fe, Al, and Si concentrations were lower in the younger than in the older soils (Table 1). From those concentrations, it was possible to calculate the allophane and ferrihydrite concentrations in the soils. The Al/Si molar ratio in the older flows was 2, indicating that Al-rich allophane was formed. This was expected in these well-drained coarse sandy soils because Parfitt (1990) found that Si concentrations are generally low in these conditions. The Al/Si molar ratio of the two younger flows was lower. We believe that the lower Al/Si ratio is mainly the result of less reliable data due to the extremely low concentrations of Al and Si, as the conditions for allophane formation in these younger flows should be similar to those in the two older flows. Therefore, we used the same conversion factor of 7 (Parfitt, 1990) to calculate the allophane concentrations in all soils.

Allophane concentrations in the soils of our study were lower (Fig. 1) than the ones from Takahashi et al. (1993) for other volcanic soils in northern California, which ranged from 7 to 146 g allophane  $\text{kg}^{-1}$  soil. Allophane concentrations in our study increased throughout the chronosequence (Fig. 1). The increase in allophane concentrations with increasing soil age was the most pronounced change observed within any of the soil properties we measured. Concentrations were up to 68 times higher in the oldest than in the youngest flow. The highest rate of change in allophane concentration occurred between the 255- and the 616-year-old soil with 0.08 (0–10 cm and 140–150 cm soil depth) to

Table 1

Bulk density of the fine soil ( $BD_{\text{fine soil}}$ ), volume of the coarse fraction ( $V_{\text{coarse fraction}}$ ), Fe, Al, and Si concentrations in the dithionate ( $Fe_d$ ), oxalate ( $Al_o$ ,  $Fe_o$ ,  $Si_o$ ), crystalline ( $Fe_{\text{cryst}}$ ), and pyrophosphate ( $Al_p$ ) extracts of the soils of the Mt. Shasta mudflow chronosequence

Soil age (year)	Soil depth (cm)	$BD_{\text{fine soil}}$ ( $g\ cm^{-3}$ )	$V_{\text{coarse fraction}}$ (%)	$Fe_d$ ( $g\ kg^{-1}$ )	$Fe_o$ ( $g\ kg^{-1}$ )	$Fe_{\text{cryst}}$ ( $g\ kg^{-1}$ )	$Al_o$ ( $g\ kg^{-1}$ )	$Al_p$ ( $g\ kg^{-1}$ )	$Si_o$ ( $g\ kg^{-1}$ )	$(Al_o - Al_p)Si_o^{-1}$ ( $mol\ mol^{-1}$ )
77	0–10	$1.34 \pm 0.18$	$15 \pm 7.6$	$1.0 \pm 0.09^*$	$1.2 \pm 0.18^*$	$0.00 \pm 0.19^*$	$0.29 \pm 0.06^*$	$0.17 \pm 0.03^*$	$0.08 \pm 0.03^*$	$1.9 \pm 0.4^*$
	10–20	$1.38 \pm 0.16$	$15 \pm 5.6$	$1.0 \pm 0.15^*$	$1.2 \pm 0.10^*$	$0.00 \pm 0.22^*$	$0.36 \pm 0.03^*$	$0.24 \pm 0.07^*$	$0.12 \pm 0.02^*$	$1.3 \pm 0.6^*$
	30–40	$1.66 \pm 0.007$	$4.0 \pm 1.3$	$1.1 \pm 0.18^*$	$1.1 \pm 0.07^*$	$0.07 \pm 0.18^*$	$0.31 \pm 0.05^*$	$0.20 \pm 0.08^*$	$0.14 \pm 0.04^*$	$1.1 \pm 0.5^*$
	70–80	$1.64 \pm 0.03$	$6.7 \pm 5.0$	$1.2 \pm 0.26^*$	$1.2 \pm 0.11^*$	$0.06 \pm 0.29$	$0.25 \pm 0.03^*$	$0.17 \pm 0.04^*$	$0.12 \pm 0.03^*$	$0.9 \pm 0.3^*$
	140–150	N.D.	N.D.	$1.1 \pm 0.23^*$	$1.2 \pm 0.17^*$	$0.00 \pm 0.36$	$0.27 \pm 0.04^*$	$0.19 \pm 0.04^*$	$0.14 \pm 0.01^*$	$0.9 \pm 0.2^*$
255	0–10	$0.98 \pm 0.15$	$14 \pm 3.8$	$2.1 \pm 0.27^*$	$1.1 \pm 0.11^*$	$0.99 \pm 0.35^*$	$1.00 \pm 0.08^*$	$0.76 \pm 0.07^*$	$0.18 \pm 0.05^*$	$1.5 \pm 0.3^*$
	10–20	$1.17 \pm 0.01$	$16 \pm 4.7$	$1.7 \pm 0.21^*$	$1.3 \pm 0.15^*$	$0.47 \pm 0.19^*$	$0.99 \pm 0.15^*$	$0.68 \pm 0.13^*$	$0.25 \pm 0.06^*$	$1.4 \pm 0.4^*$
	30–40	$1.35 \pm 0.15$	$23 \pm 6.7$	$1.8 \pm 0.24^*$	$1.2 \pm 0.10^*$	$0.58 \pm 0.19^*$	$0.73 \pm 0.28^*$	$0.47 \pm 0.22^*$	$0.22 \pm 0.05^*$	$1.4 \pm 0.7^*$
	70–80	$1.47 \pm 0.05$	$15 \pm 2.7$	$1.8 \pm 0.27^*$	$1.2 \pm 0.19^*$	$0.57 \pm 0.39$	$0.49 \pm 0.14^*$	$0.27 \pm 0.17^*$	$0.21 \pm 0.04^*$	$1.3 \pm 0.4^*$
	140–150	N.D.	N.D.	$1.4 \pm 0.55^*$	$1.3 \pm 0.24^*$	$0.07 \pm 0.45$	$0.57 \pm 0.17^*$	$0.23 \pm 0.11^*$	$0.26 \pm 0.06^*$	$1.5 \pm 0.3^*$
616	0–10	$0.82 \pm 0.11$	$14 \pm 5.3$	$3.1 \pm 0.25^*$	$1.8 \pm 0.13^*$	$1.25 \pm 0.25^*$	$12.0 \pm 2.4^*$	$4.1 \pm 0.72^*$	$4.1 \pm 1.2^*$	$2.0 \pm 0.1^*$
	10–20	$0.92 \pm 0.11$	$13 \pm 5.3$	$3.0 \pm 0.40^*$	$2.0 \pm 0.07^*$	$1.05 \pm 0.38^*$	$13.3 \pm 2.6^*$	$2.8 \pm 0.58^*$	$5.3 \pm 1.0^*$	$2.1 \pm 0.2^*$
	30–40	$1.04 \pm 0.003$	$15 \pm 7.3$	$3.1 \pm 0.62^*$	$2.3 \pm 0.22^*$	$0.83 \pm 0.50^*$	$14.3 \pm 4.4^*$	$1.7 \pm 0.55^*$	$7.2 \pm 2.1^*$	$1.8 \pm 0.1^*$
	70–80	$0.94 \pm 0.01$	$29 \pm 19$	$2.7 \pm 0.72^*$	$2.5 \pm 0.19^*$	$0.15 \pm 0.67$	$12.0 \pm 0.9^*$	$0.88 \pm 0.47^*$	$6.2 \pm 1.6^*$	$2.0 \pm 0.8^*$
	140–150	N.D.	N.D.	$1.8 \pm 0.91^*$	$2.3 \pm 0.56^*$	$0.00 \pm 0.54$	$7.0 \pm 3.5^*$	$0.65 \pm 0.43^*$	$4.1 \pm 2.6^*$	$1.6 \pm 0.1^*$
~ 1200+	0–10	$0.93 \pm 0.132$	$8.1 \pm 4.1$	$3.1 \pm 0.54^*$	$1.8 \pm 0.37^*$	$1.23 \pm 0.24^*$	$9.9 \pm 4.0^*$	$3.7 \pm 1.2^*$	$3.0 \pm 1.1^*$	$2.1 \pm 0.3^*$
	10–20	$0.99 \pm 0.17$	$12 \pm 7.8$	$2.9 \pm 0.48^*$	$2.1 \pm 0.42^*$	$0.82 \pm 0.24^*$	$12.4 \pm 5.6^*$	$3.5 \pm 1.5^*$	$4.4 \pm 1.8^*$	$2.0 \pm 0.3^*$
	30–40	$0.97 \pm 0.01$	$7.5 \pm 2.9$	$3.3 \pm 0.46^*$	$2.5 \pm 0.34^*$	$0.89 \pm 0.42^*$	$15.8 \pm 4.1^*$	$2.2 \pm 0.64^*$	$6.7 \pm 1.8^*$	$2.1 \pm 0.1^*$
	70–80	$1.06 \pm 0.01$	$17 \pm 5.9$	$3.2 \pm 0.24^*$	$2.6 \pm 0.21^*$	$0.63 \pm 0.36$	$15.7 \pm 2.2^*$	$1.3 \pm 0.09^*$	$8.3 \pm 1.3^*$	$1.8 \pm 0.1^*$
	140–150	N.D.	N.D.	$2.1 \pm 0.37$	$2.4 \pm 0.35^*$	$0.00 \pm 0.30$	$8.7 \pm 4.6^*$	$0.88 \pm 0.25^*$	$4.7 \pm 2.9^*$	$1.8 \pm 0.1^*$

\*Indicates significant differences ( $P < 0.05$ ) among soils from the four different ages at a particular depth using ANOVA. N.D. indicates not determined.

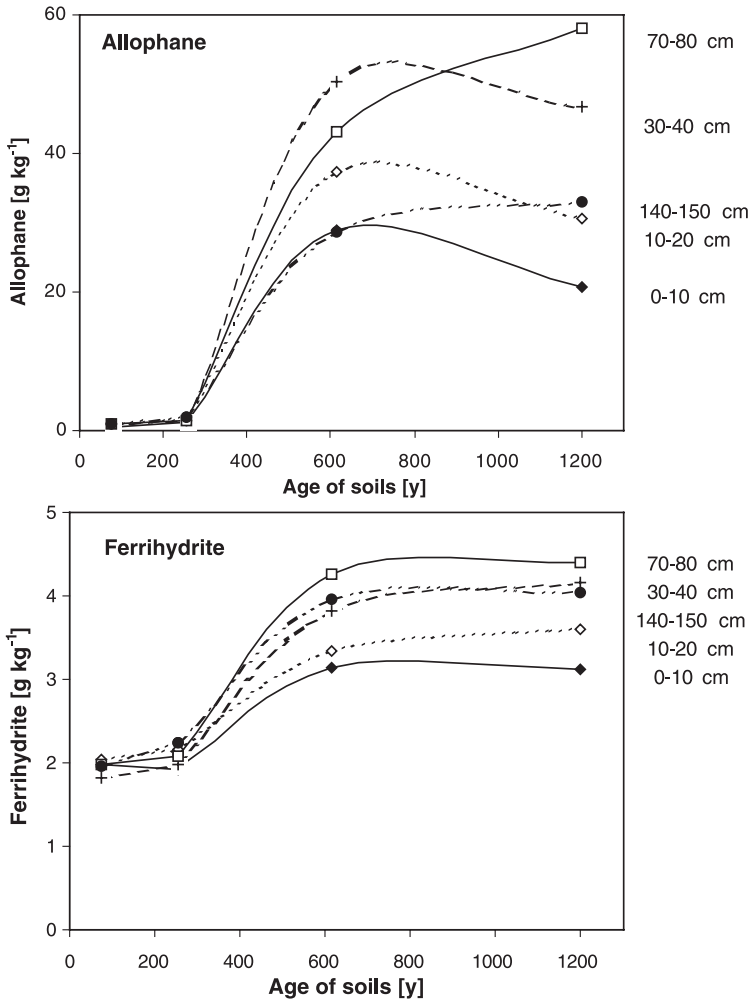


Fig. 1. Allophane and ferrihydrate accretion during the first ~ 1200 years of soil formation.

0.14 (30–40 cm soil depth) g allophane kg<sup>-1</sup> year<sup>-1</sup>. The high rate of change in allophane concentration in the deeper soil may be partly due to the fact that allophane can be formed from percolating solutions.

In the Mt. Shasta chronosequence, ferrihydrate concentrations only increased by a factor of 2.3 from the youngest to the oldest flow (Fig. 1). Dickson and Crocker (1954) reported that the concentrations of pedogenic Fe (Fe<sub>d</sub>) concentrations were higher in the two older than in the two younger flows but that there was no particular relation with age within the two groups. However, our data showed a trend of increasing Fe<sub>d</sub> concentrations from the A to the D flow soils at all depths (Table 1). Concentrations of crystalline Fe oxides were low (<1.3 g Fe kg<sup>-1</sup>) in all flows. However, at 0–10-, 10–20-, and 30–40-cm soil depth, concentrations were significantly higher in the two older than in the two younger flows.

With increasing soil development, the specific surface area increased by a factor of up to 2.6 from the youngest to the oldest flow (Fig. 2). The specific surface area of allophane determined with the EGME method was reported by Wada (1989) to be 435 to 534  $\text{m}^2 \text{g}^{-1}$ . The specific surface area of ferrihydrite was determined by Schwertmann and Taylor (1989) to be 2–5  $\text{m}^2 \text{g}^{-1}$ . These specific surface areas can be used to estimate the contributions of allophane and ferrihydrite to the total specific surface area in our soils. The increase in surface area over time attributable to allophane and ferrihydrite is

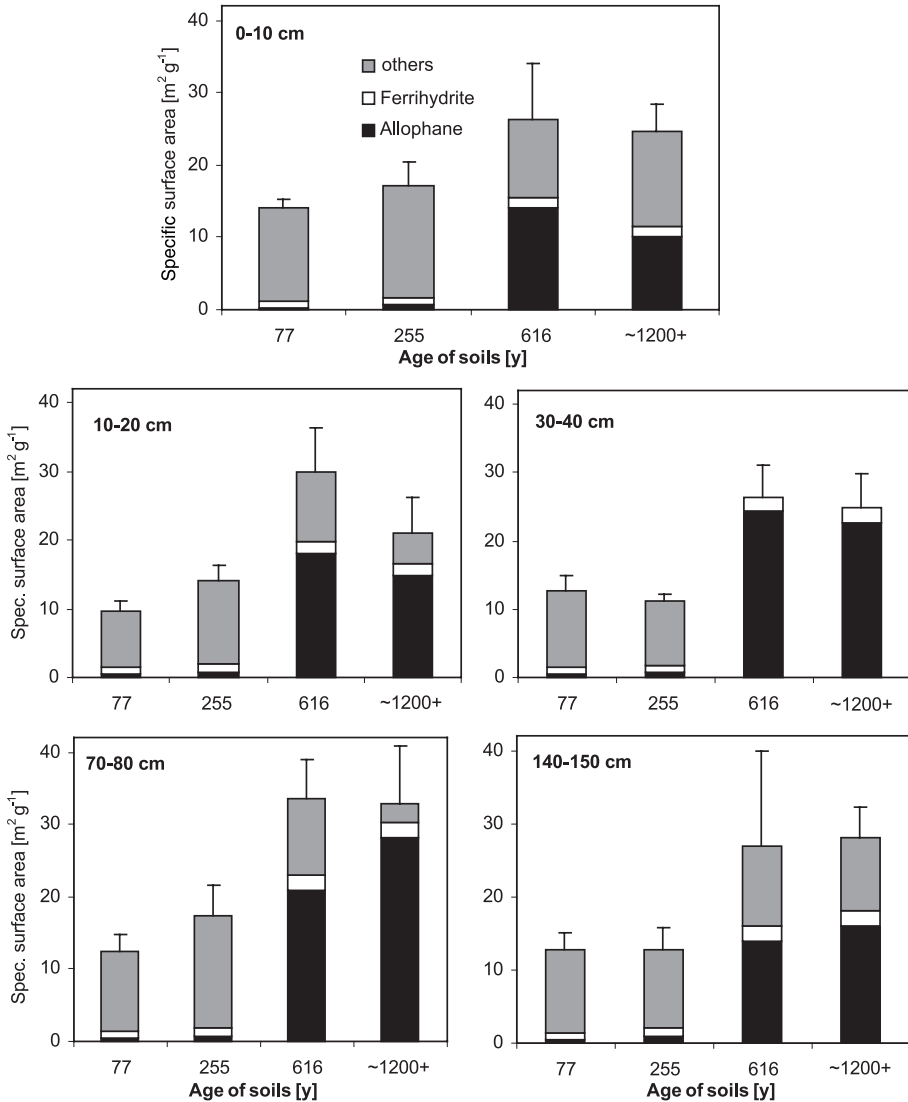


Fig. 2. Measured total specific surface area and calculated specific surface area of allophane and ferrihydrite in the soil.

consistent with most of the observed increase in total surface area over time. The contribution of allophane to the total specific surface area in the A flow was small (2–4%), whereas in the E flow it was between 41% and 97% of the total specific surface area (Fig. 2). The contribution of allophane to the surface area in the topsoil was smaller than in the deeper soil because organic matter also contributed to the surface area. The contribution of the ferrihydrite concentrations to the total specific surface area ranged between 6% and 11% for all flows and all soil depths. This range was smaller because the increase in ferrihydrite concentrations with increasing soil age was less pronounced than for the allophane concentrations. That the allophane concentrations increased to a larger extent than the total specific surface area indicated a change in the character of the surface area. The fact that the activity of the surface area changed is important in predicting sorption characteristics of phosphate and dissolved organic matter of the soil because the surface of allophane is more active and therefore adsorbs these species more strongly than the same surface area of andesitic sand. The chief mechanism for adsorption of phosphate and the carboxyl groups of dissolved organic matter to allophane is through ligand exchange rather than simple electrostatic attraction to anion exchange sites (Rajan, 1975; Parfitt et al., 1977; Wershaw et al., 1996). Consequently, in these soils the allophane concentrations are a much better predictor of sorption in the soil than the surface area.

The specific surface areas attributed to other sources besides allophane and ferrihydrite do not show a consistent trend with the age of soil. There is considerable variability in this fraction, probably due to the analytical variability in determining the relatively small surface area of these soils and because of the assumptions in attributing the surface area to different components. The surface areas of these other components are likely due to the silt and sand-sized fractions of the parent material, and in the upper depths, to organic matter.

### 3.2. Organic matter accretion

Concentrations of organic C and N increased with increasing soil age and decreased with increasing soil depth (Fig. 3). In the youngest soil, C and N concentrations in the surface soil were only slightly higher than in the deeper soil. Carbon and N concentrations at 0–10-cm soil depth increased significantly during the first 600 years of soil formation but then remained similar between 600 and ~ 1200 years. From the youngest to the oldest soil, concentrations of C increased by a factor of 6 to 26, and those of N increased by a factor of 5 to 10. Carbon and N concentrations in the three older flows were similar to those reported by Dickson and Crocker (1953b) and Sollins et al. (1983) who sampled in 1951 and 1979, respectively. In the youngest mudflow, we had the opportunity to compare the development of the surface soil over time because Dickson and Crocker (1953b) analyzed the soil at age 27 years, Sollins et al. analyzed the soil at age 55 years, and we analyzed the soil at age 77 years. The combination of the data from the repeated sampling in the youngest flow in 1951 (Dickson and Crocker, 1953b), 1979 (Sollins et al., 1983), and 2001 (our study) with the chronosequence study of the older flows gave us the possibility of examining C and N concentrations in 27-, 55-, 77-, 255-, 616-, and approximately 1200+-year-old soils. The 0–10-cm depth offered the best comparison of C and N concentrations (Fig. 4), as all authors

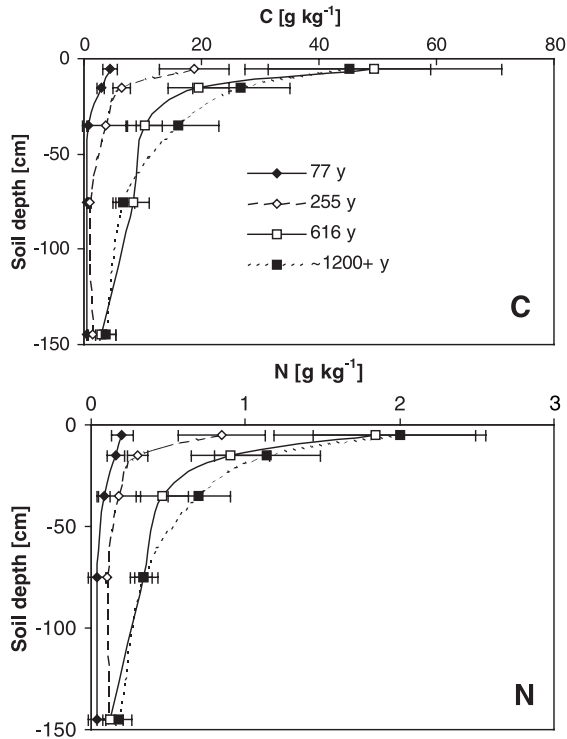


Fig. 3. Carbon and N concentrations in the 77-, 255-, 616-, and ~ 1200+-year-old soils.

studied the same depth (except for Dickson and Crocker, 1953b: 0–13 cm). In addition, this depth was interesting because it gave us the opportunity to measure the rate of development of an A horizon. Carbon and N concentrations showed a linear increase with increasing soil age over the first ~ 600 years. Afterwards, C and N concentrations in the 0–10-cm depth appeared to reach an equilibrium.

We also calculated the C and N stocks in the different soils. For a better comparison with the data of Sollins et al. (1983), we chose the same soil depth (0–70 cm) as Sollins et al. (1983) and used the bulk density of the fine soil and volume of the coarse fraction given in Table 1. Fig. 5 shows the C and N stocks over time. The slopes of the regression line, which can be interpreted as accretion rates, showed a C accretion rate for the first 600 years of  $139 \text{ kg C ha}^{-1} \text{ year}^{-1}$  and an N accretion rate of  $5.3 \text{ kg N ha}^{-1} \text{ year}^{-1}$ . The calculations of these accretion rates were based on time series analysis and did not require assumptions about the C and N content of the parent material. Consequently, these estimates of accretion rates are more reliable than previous estimates for this chronosequence. Additionally, the N accretion rates were within the  $5\text{--}10 \text{ kg N ha}^{-1} \text{ year}^{-1}$  range suggested by Binkley et al. (2000). We did not include the data of the approximately 1200+-year-old soil in the regression because the age of this soil was not known exactly. The C and N concentrations at 0–10 cm seemed to have reached equilibrium after ~ 600 years, as there was no significant difference ( $P > 0.05$ ) in C and N concentration between

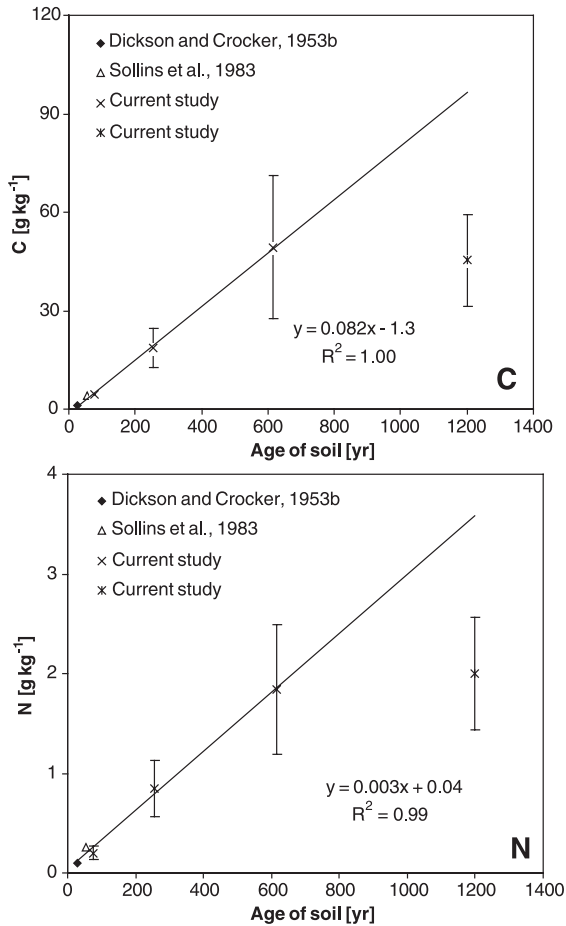


Fig. 4. Carbon and N concentrations in the 0–10 cm soil depth as a function of soil age. The figure contains data from Dickson and Crocker (1953b) and Sollins et al. (1983). Carbon and N concentrations in the ~ 1200+-year-old soil were not included in the regression.

the 600- and the 1200+-year-old soil (Fig. 3). However, the N stock at 0–70-cm depth was still significantly increasing after 600 years (Fig. 5). The difference in the C stocks of the 600- and the 1200+-year-old soils was only of borderline significance ( $P=0.10$ ). The deepening of the distribution of C and N in the oldest soil was the main reason for the continued accretion in the oldest soil (Fig. 3).

### 3.3. Effective CEC and pH

Changes in mineralogy and organic matter accretion affected the  $CEC_{\text{eff}}$  and pH of the soils. Whereas the  $CEC_{\text{eff}}$  in the 77-year-old soil did not change significantly ( $P>0.05$ , ANOVA) with soil depth, it significantly decreased with increasing soil depth

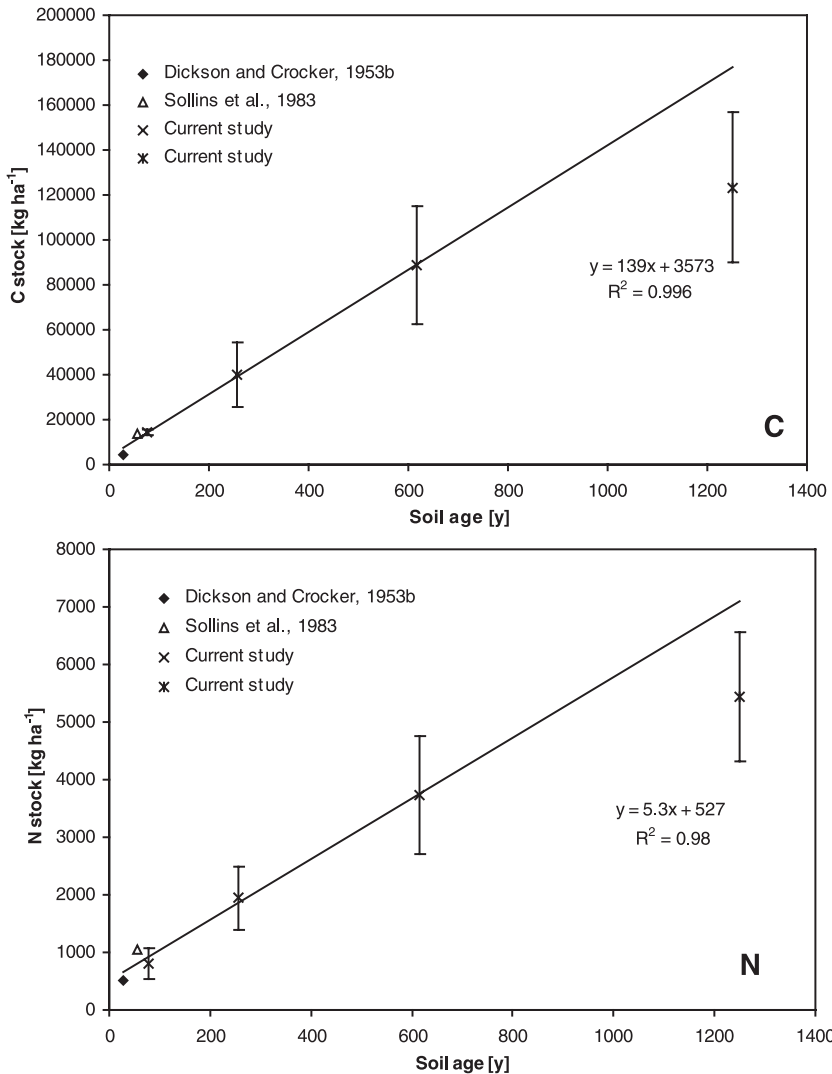


Fig. 5. Carbon and N stocks at 0–70 cm soil depth as a function of soil age. The figure contains data from Dickson and Crocker (1953b) and Sollins et al. (1983). Carbon and N concentrations in the ~ 1200+-year-old soil were not included in the regression.

in all of the three older soils. In addition,  $CEC_{eff}$  was between three and four times higher at 0–10 cm than at 140–150-cm soil depth in the three older soils (Fig. 6). With increasing soil age, the  $CEC_{eff}$  increased significantly ( $P < 0.05$ ) by a factor of 5 at 0–10-cm soil depth, but only differed by a factor of 1.2 (difference not significant,  $P > 0.05$ ) at 140–150-cm soil depth. While the overall  $CEC_{eff}$  of these soils was relatively low, the tendency for leaching of cationic nutrients is likely to decrease with increasing soil age.

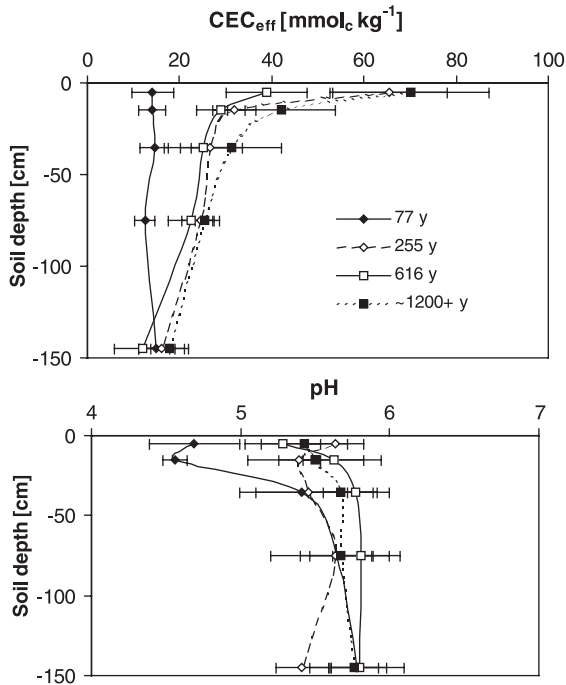


Fig. 6. Effective cation exchange capacity ( $CEC_{\text{eff}}$ ) and soil pH in the 77-, 255-, 616-, and ~ 1200+-year-old soils.

The pH of the soils varied from about 4.6 to 5.8. Soil pH in the surface soil was lowest in the 77-year-old soil, perhaps due to the fact that the vegetation was largely *Pinus ponderosa* in the 77-year-old soil whereas it was mixed oak, fir, and cedar in the other flows (Fig. 6). In a study by Wada (1980), the pH at the point of zero charge for a B horizon containing allophane was 6.3. The allophane in this soil had an Al/Si ratio of 2:1, which was similar to that in our soils. Since our soil pH was below the point of zero charge of allophane, it is likely that the allophane in our soils had net positive charge. Consequently, allophane contributes only very little to the measured effective CEC which is likely to be mainly attributable to organic matter in the surface soil and other minerals in the subsurface horizons. A regression of  $CEC_{\text{eff}}$  vs. C concentration across all sites and all depths was highly significant ( $P < 0.001$ ,  $r^2 = 0.59$ ,  $CEC_{\text{eff}} = 0.88 C + 17$ ).

#### 4. Conclusions

Soil and climatic conditions in the Mt. Shasta mudflow chronosequence lead to the formation of Al-rich allophane. Allophane concentrations increased with a rate of up to  $0.14 \text{ g ka}^{-1} \text{ year}^{-1}$  while ferrihydrite accumulated at a rate of only  $0.004 \text{ g kg}^{-1} \text{ year}^{-1}$ . Even in the oldest soil, concentrations of crystalline Fe oxides were less than  $1.3 \text{ g kg}^{-1}$ .

Specific surface area in the youngest soil was low and originated mainly from andesitic sand. In the oldest flow, surface area was up to 2.6 times higher than in the youngest soil and 41–97% of the surface area could be attributed to allophane. Organic matter accumulated with a rate of  $139 \text{ g C kg}^{-1} \text{ ha}^{-1} \text{ year}^{-1}$  and  $5.3 \text{ g N kg}^{-1} \text{ ha}^{-1} \text{ year}^{-1}$  over the first ~ 600 years. Increases in organic matter concentrations with soil development also lead to increases in CEC, which indicates an improved ability of the soil to adsorb and retain nutrients in the ecosystem.

## Acknowledgements

We are grateful to Peter Van Susteren of the U.S. Forest Service, McCloud Ranger District, without whose help this study would not have been possible. This study was funded by the National Science Foundation, Award #9974062. Research was supported in part by the Nevada Agricultural Experiment Station.

## References

- Baker, A.S., Kuo, S., Chae, Y.M., 1981. Comparison of arithmetic average soil pH values with the pH values of composite samples. *Soil Sci. Soc. Am. J.* 45, 828–830.
- Binkley, D., Son, Y., Valentine, D.W., 2000. Do forests receive occult inputs of nitrogen? *Ecosystems* 3, 321–331.
- Carter, D.L., Mortland, M.M., Kemper, W.D., 1986. Specific surface. In: Klute, A. (Ed.), *Methods of Soil Analyses: Part 1. Physical and Mineralogical Methods*. Agronomy Monograph, pp. 413–423.
- Dahlgren, R.A., 1994. Quantification of allophane and imogolite. *Quantitative Methods in Soil Mineralogy*. SSSA, Madison, WI, pp. 430–451.
- Dickson, B.A., Crocker, R.L., 1953a. A chronosequence of soils and vegetation near Mt Shasta, California: I. Definition of the ecosystem investigated and features of the plant succession. *J. Soil Sci.* 4, 123–141.
- Dickson, B.A., Crocker, R.L., 1953b. A chronosequence of soils and vegetation near Mt Shasta, California: II. The development of the forest floor and the carbon and nitrogen profiles of the soils. *J. Soil Sci.* 4, 142–156.
- Dickson, B.A., Crocker, R.L., 1954. A chronosequence of soils and vegetation near Mt Shasta, California: III. Some properties of the mineral soil. *J. Soil Sci.* 5, 173–191.
- Glauser, R., 1967. The ecosystem approach to the study of the Mt Shasta mudflows. Dissertation. University of California, Berkeley, California, USA.
- Holmgren, G.G.S., 1967. A rapid citrate–dithionate extractable iron procedure. *Soil. Sci. Soc. A. Proc.* 31, 210–211.
- Hugget, R.J., 1998. Soil chronosequences, soil development, and soil evolution: a critical review. *Catena* 32, 155–172.
- Jenny, H., 1980. The soil resource. Origin and Behavior. *Ecological Studies*, vol. 37. Springer, New York. 337 pp.
- McKeague, J.A., 1967. An evaluation of 0.1 M pyrophosphate and pyrophosphate–dithionate in comparison with oxalate as extractants of the accumulation products in podzols and some other soils. *Can. J. Soil Sci.* 47, 95–99.
- Meko, D.M., Therrel, M.D., Baisan, C.H., Hughes, M.K., 2001. Sacramento River flow reconstructed to A.D. 869 from tree rings. *J. Am. Water Resour. As.* 37, 1029–1039.
- Nieuwenhuys, A., Verburg, P.S.J., Jongmans, A.G., 2000. Mineralogy of a soil chronosequence on andesitic lava in humid tropical Costa Rica. *Geoderma* 98, 61–82.
- Parfitt, R.L., 1990. Allophane in New Zealand—a review. *Aust. J. Soil Res.* 28, 343–360.
- Parfitt, R.L., Childs, C.W., 1988. Estimation of forms of Fe and Al: A review, and analysis of contrasting soils by dissolution and Moesbauer methods. *Aust. J. Soil Res.* 26, 121–144.

- Parfitt, R.L., Kimble, J.M., 1989. Conditions for formation of allophane in soils. *Soil Sci. Soc. Am. J.* 53, 971–977.
- Parfitt, R.L., Fraser, A.R., Farmer, V.C., 1977. Adsorption on hydrous oxides: III. Fulvic acid and humic acid on goethite, gibbsite, and imogolite. *J. Soil Sci.* 28, 289–296.
- Rajan, S.S.S., 1975. Mechanism of phosphate adsorption by allophanic clays. *N.Z. J. Sci.* 18, 93–101.
- Schlesinger, W.H., 1997. *Biogeochemistry Analysis of Global Change*, 2nd ed. Academic Press, San Diego, CA.
- Schwertmann, U., 1964. Differenzierung der Eisenoxide des Bodens durch Extraktion mit saurer Ammoniumoxalatlösung. *Z. Pflanzenemähr. Bodenk.* 105, 194–202.
- Schwertmann, U., Taylor, R.M., 1989. Iron oxides. In: Dixon, J.B., Weed, S.B. (Eds.), *Minerals in Soil Environment*. Soil Sci. Soc. of America, Madison, WI, USA, pp. 379–438.
- Sollins, P., Spycher, G., Topik, C., 1983. Processes of soil organic matter accretion at a mudflow chronosequence, Mt Shasta, California. *Ecology* 64, 1273–1282.
- Sumner, M.E., Miller, W.P., 1996. Cation exchange capacity and exchange coefficients. In: Sparks, D.L., et al. (Eds.), *Methods of Soil Analysis: Part 3. Chemical Methods*. American Society of Agronomy, Madison, WI, pp. 1201–1229.
- Takahashi, T., Dahlgren, R., van Susteren, P., 1993. Clay mineralogy and chemistry of soils formed in volcanic materials in the xeric moisture regime of northern California. *Geoderma* 59, 131–150.
- Wada, K., 1980. Mineralogical characteristics of Andosols. In: Keng, B.K.G. (Ed.), *Soils with Variable Charge*. N.Z. Soc. Soil Sci., pp. 87–107. Lower Hutt, New Zealand.
- Wada, K., 1989. Allophane and imogolite. In: Dixon, J.B., Weed, S.B. (Eds.), *Minerals in Soil Environment*. Soil Sci. Soc. of America, Madison, WI, pp. 1051–1087.
- Wershaw, R.L., Llaguno, E.E., Leenheer, J.A., 1996. Mechanisms of formation of humus coatings on mineral surfaces: 3. Composition of adsorbed organic acids from compost leachate on alumina by solid-state  $^{13}\text{C}$  NMR. *Colloids Surf., A, Physicochem. Eng. Asp.* 108, 213–223.